www.jcimcr.org

JCIMCR OPEN ACCESS Journal of Clinical Images and Medical Case Reports

ISSN 2766-7820

Case Report

Open Access, Volume 2

Diagnosis of atypical mass-forming chronic pancreatitis mimicking pancreatic carcinoma: A case report

Han-Yue Wang; Hao-Su Huang; Meng Wang; Jie Peng*

Department of Gastroenterology, Xiangya Hospital of Central South University, Changsha 410008, Hunan Province, China.

***Corresponding Author: Jie Peng**

Department of Gastroenterology, Xiangya Hospital of Central South University, Xiangya road, Changsha 410008, Hunan Province, China.

Email: pengjie2014@csu.edu.cn

Received: Aug 28, 2021

Accepted: Oct 01, 2021

Published: Oct 08, 2021

Archived: www.jcimcr.org

Abbreviations: MFCP: Mass-Forming Chronic Pancreatitis; PC: Pancreatic Carcinoma; CP: Chronic Pancreatitis; Tbil: Total Bilirubin; Dbil: Direct Bilirubin; MRI: Magnetic Resonance Imaging; MRCP: MR Cholangiopancreatography; CT: Computed Tomography; ERCP: Encoscopic Retrograde Cholangio-Pancreatography; EUS-FNA: Endoscopic Ultrasonography Guided Fine-Needle Aspiration; CA 19-9: Carbohydrate Antigen 19-9; SUV: Standardised Uptake Value; 18-FDG-PET / CT: 18F-FDG Positron Emission Tomography (PET)/CT.

Abstract

Background: Mass-Forming Chronic Pancreatitis (MFCP) is rare. Moreover, atypical MFCP is difficult to differentiate from Pancreatic Carcinoma (PC) in clinical manifestations, laboratory, and imaging examinations. Diagnosis could be supported by the pathological findings of focal inflammatory fibrosis without evidence of tumor in the pancreas.

Case summary: A 52-year-old man had acute pancreatitis twice over 7 months. Amylase and lipase levels were three times higher than the normal range without any clinical symptoms. At the 6th month, the patient lost 15 kg of weight, and abdominal ultrasonography revealed pancreatic head space occupied. All the findings in multimodal imaging including computed tomography image, Magnetic Resonance (MR) imaging with MR cholangiopancreatography, and 18F-FDG positron emission tomography/computed tomography showed an irregular nodule with low density, low signal, and low echo in the head of the pancreas, which were lower than those in the normal pancreatic tissue. The proximal main pancreatic duct was truncated and stenosed, and the distal duct was dilated. Subsequently, he developed progressive painless jaundice, and the specific tumor marker levels were increased. Most of these manifestations were suggestive of the pancreatic malignant tumor; however, multiple specimen pathological findings obtained from laparotomy and endoscopic ultrasonography-guided fine-needle aspiration revealed focal chronic inflammation, fibrosis, and necrosis.

Conclusion: This report describes a case of atypical MFCP mimicking PC at clinical presentation and laboratory findings, especially in multimodal imaging. However, the combination of atypical multimodal imaging features, which support MFCP rather than PC, and endoscopic ultrasonography-guided fine-needle aspiration are useful for improving the diagnostic rate of atypical MFCP and avoiding unnecessary surgery.

Keywords: pancreatic carcinoma; mass-forming chronic pancreatitis; pancreatic head space occupying; diagnosis; multimodal imaging.

Citation: Wang HY, Huang HS, Wang M, Peng J. Diagnosis of atypical mass-forming chronic pancreatitis mimicking pancreatic carcinoma: A case report. J Clin Images Med Case Rep. 2021; 2(5): 1350.

Introduction

Pancreatic Carcinoma (PC) is the fourth leading cause of cancer-related deaths worldwide, with ductal adenocarcinoma and its variants accounting for over 90% of the cases, with an overall mean 5-year survival rate of 8% and a mean survival rate of 32% for localized disease [1]. Although the Whipple procedure offers an improved survival rate for patients with localized resectable disease (mortality rate, <5%), morbidity from the Whipple procedure can be as high as 40–50%, which makes preoperative identification of non-neoplastic pancreatic masses important [2,3].

Chronic Pancreatitis (CP) is a disease of recurrent or ongoing prolonged pancreatic inflammation, which is characterized by the development of irreversible morphological and functional abnormalities. Although atrophy is one of the main features of CP, mass-like focal enlargement of the pancreatic parenchyma may occasionally occur in the pancreatic head, which is called Mass-Forming Chronic Pancreatitis (MFCP). However, it remains difficult to distinguish MFCP from a dismal PC because imaging findings, clinical presentation, risk factors, and laboratory evaluation overlap in patients with pancreatic inflammatory processes and those with a pancreatic neoplasm [4,5]. To further complicate this issue, CP may develop into PC, which may lead to obstructive chronic pancreatitis secondary to pancreatic ductal obstruction [6].

Although pathology is the gold standard for differentiating MFCP from PC, special identification features on multimodal imaging are of great clinical significance for MFCP diagnosis in this case. Herein, we report an interesting case of atypical MFCP mimicking PC at clinical presentation, laboratory findings, and multimodal imaging features.

Case presentation

Written informed consent was obtained prior to imaging allowing the presentation of this case and data. A 52-year-old man was admitted to our department with a 7-month history of continuously elevated amylase and findings of the pancreatic space-occupying lesion in the pancreatic head space for 1 month. In the first three months, he was admitted to the hospital for severe abdominal pain and was diagnosed with acute pancreatitis twice. Laboratory findings, including liver transaminase, total bilirubin (TBiL), and direct bilirubin (DBiL) levels, as well as tumor markers were within the normal range, except for amylase and lipase values that were exceeding normal range 3 times at every measurement. Enhanced computed Tomography (CT) of the pancreas showed peripancreatic inflammatory exudation, and the pancreatic duct was not dilated. After treatment with anti-inflammatory agents for a month, magnetic resonance imaging (MRI) with MR Cholangiopancreatography (MRCP) showed no definite abnormal signal emanating from the head of the pancreas and pancreatic duct (Figure 1A). However, the amylase level remained high after several periodic measurements, while he had neither abdominal pain, nor hectic fever, night sweating, cutaneous or scleral icterus, loss of appetite, nausea, or distaste for oil. The patient had no previous history of alcohol abuse, gallbladder stones, hyperlipidemia, overeating, etc., and the imaging examination excluded biliary tract diseases. There was no family history, including relevant genetic information.

The patient lost 15 kg of weight within 6 months, and the amylase level had never dropped to normal. To establish the definitive diagnosis, abdominal ultrasonography was performed which showed that the head of the pancreas was enlarged, and provided acoustic images of hypoechoic nodules and a dilated main pancreatic duct (Figure 4D,E). The serological examination showed elevated serum amylase and lipase levels (amylase, 149.5U/L; lipase, 232.7U/L), while no abnormalities were observed in serum bilirubin, transaminase, immunoglobulin IgG4, and the tumor markers carbohydrate antigen 19-9 and 125 (CA19-9 and CA125). On MRI, the lesion displayed a long-T1 and equal-T2 signal, with a size of approximately 26 X 28 mm, which was lower than that of normal pancreatic tissue after contrast administration. MRCP showed proximal truncation and distal expansion of the pancreatic duct, and no stones were found in the gallbladder and common bile duct (Figure 1B). 18F-FDG positron emission tomography (PET)/CT showed a nodular abnormal radioactive concentration with a size of 27 X 19 mm in the sulcus process in the head of the pancreas, the standardized uptake value (SUVmax) was 12.6, and a slightly lower-density nodule shadow was found on CT of the corresponding part. The tail of the pancreas showed patchy radioactive concentration, SUVmax value was 4.0, and the pancreatic duct was dilated, while no abnormal radioactive concentration and enlarged lymph nodes were found in the retroperitoneum. Considering the high possibility of pancreatic carcinoma, pancreaticoduodenectomy was performed. An interesting phenomenon was found after laparotomy, in which the whole pancreas was hardened and closely related to the surrounding tissues and superior mesenteric arteries and veins. The original operation was difficult to perform, so a wedge-shaped tissue of the enlarged pancreatic head and part of the transverse colon mesentery were further removed for pathological biopsy. The results of postoperative pathological examination showed chronic inflammation in the pancreatic head, with no large amount of plasma cell infiltration (Figure 2A,B).

More than 2 months after the operation, the patient developed progressive weight loss and cutaneous or scleral icterus, without chills, fever, and abdominal pain. Physical examination revealed a mass around the umbilicus, with soft texture and mild tenderness, and no obvious tenderness or rebound pain in the abdomen. His laboratory findings showed that serum albumin was 28.5 g/L (normal range: 40.0-50.0 g/L), TBiL 34.9 umol/L (1.7-17.1 umol/L), DBiL 22.3 umol/l (0.0-6.8 umol/l), glutamic pyruvic transaminase 78.3 u/l (9.0-50.0 u/L), and glutamyltranspeptidase (GGT) 133.7 u/ L (10.0-60.0 u/L). The CA125 was 60.09u/mL (0-35 u/mL) and CA19-9 12.11 u/mL (0-35 u/mL). Meanwhile, the anti-SMA, anti Ro52, anti-SLA/LP, anti LC-1, anti gp210, anti LKM-1, anti Sp100, anti AMA-M2, and anti M2-3E (BPO) antibodies were all negative. In peritoneal drainage fluid, the Rivalta test was positive, the total number of cells was 1300 X 10^6/L, adenosine deaminase was 67.3 u/L, and amylase was up to 55024 U/L, which could diagnose pancreatic ascites comprehensively. Within a week, the bilirubin and GGT levels were gradually increased, jaundice was progressively aggravated, and electronic gastroscopy showed duodenal bulb stenosis (Figure 4F). The reexamination of abdominal enhanced CT showed that the largest layer of the pancreatic head mass was approximately 46 X 32 mm. The attenuations of mass at the plane scanning (54 HU), arterial phase (63 HU), and portal venous phase (85

HU) were slightly lower than the surrounding pancreatic tissue (Figure 3A-C). The pancreatic body and tail were slightly atrophied, and the main pancreatic duct was slightly dilated. The widest diameter of the common bile duct was approximately 19 mm, accompanied by a slightly dilated pancreatic duct and intrahepatic bile duct. Multiple inflammatory exudation and peripheral pseudocyst formation were observed around the pancreas (Figure 3D-J). To further clarify the diagnosis, the patient underwent diagnostic endoscopic ultrasound-guided fine-needle aspiration (EUS-FNA) of the mass (Figure 4A-C). Under the guidance of endoscopic ultrasonography, biopsy tissues were obtained by several punctures at different locations of the pancreatic head nodules, and the final pathology still suggested a large number of inflammatory cell infiltrates (Figure 2C-E). The final diagnosis of the presented case was mass-forming chronic pancreatitis (MFCP). The patient had obstructive jaundice due to compression of the common bile duct in the head of the pancreas. The patient's jaundice was getting worse and liver function was clearly abnormal: serological testing of TBiL (250.8 umol/L), DBiL (195.8 umol/L), glutamic pyruvic transaminase (70.5 U/L), GGT (161.8 U/L), CA19-9 (487.37 U/mL), CA125 (63.56 U/mL), amylase and lipase all elevated progressively. To relieve the obstruction, endoscopic retrograde cholangiopancreatography (ERCP) was used to insert the biliary stent. Duodenal bulb stenosis was observed when the electronic gastroscope reached the duodenum (Figure 4F). Although it is difficult for the gastroscope to pass through the stenosis right along, it has finally reached the duodenal nipple. Intraoperative endoscopic retrograde cholangiography showed dilatation of the middle and upper segments of the common bile duct, and no development of the lower segment. Then, a metal stent was smoothly placed under the guide wire.

At the follow-up visit, one month after ERCP biliary stenting, the patient's jaundice disappeared, and the TBiL, DBiL, transaminase, and tumor marker CA19-9 levels were decreased to normal. However, the levels of amylase and lipase were still high. Abdominal CT showed that the size and features of the mass in the head of the pancreas were the same as before. The exudation of the right paracolonic sulcus disappeared, and there was still an encapsulated effusion in the abdominal cavity. Two months after hospital discharge, the patient still experienced recurrent paroxysmal distending pain around the umbilicus with occasional diarrhea, without nausea, vomiting, oil aversion, anorexia, hematochezia, and a weight drop of approximately 5 kg before discharge. Repeated checks of amylase and lipase levels showed more than 3 times higher than that of the normal range. We informed the patient that MFCP has the risk of developing a pancreatic cancer, and recommended that regular monitoring of abdominal enhanced CT and tumor markers should be conducted to track the changes in pancreatic head mass.

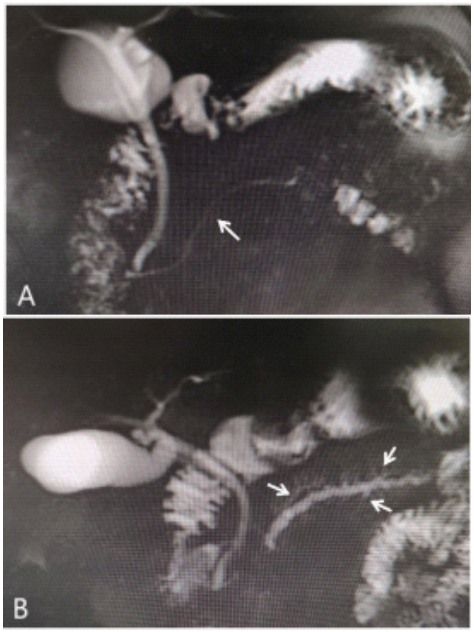

Figure 1: (A). MRCP showed no definite abnormal signal from the head of pancreas, and the common bile duct and the main pancreatic duct were in normal shape.
(B). At the 6th month of the course, MRCP showed the proximal main pancreatic duct was truncated and stenosed, and the distal was dilated without visualisation of the pancreatic duct throughout the mass. Although duct-penetrating sign is negative, there were collateral branch ducts dilatation in the distal pancreas (white arrows). Meanwhile, there were no exterior and interior cholangiectasis of liver.

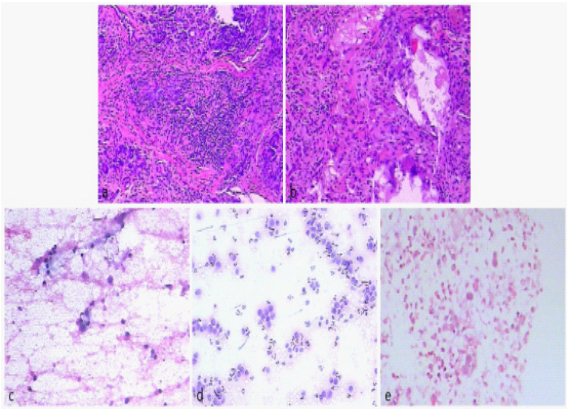

Figure 2: (a,b) Biopsy specimens of pancreatic head mass and mesocolon transversum which were obtained by laparotomy:
(a) Pancreatic tissue showed chronic inflammatory changes, fibrous tissue hyperplasia and chronic inflammatory cell infiltration. (**b**) There was necrosis of fat tissue in mesentery of transverse colon with giant cell granuloma reaction.
(c,d,e) Specimens of the mass which obtained from EUS-FNA several punctures at different places of pancreatic head nodules. **(c,d)** The tissue smear and basal fluid cytology of pancreatic tissue showed there were histiocytes, lymphocytes and neutrophils. **(e)** Pathology slice showed a few broken, degenerated and necrotic tissue, with more inflammatory cell infiltrated, and no clear evidence of malignancy.

Figure 3 Findings from computed tomography.

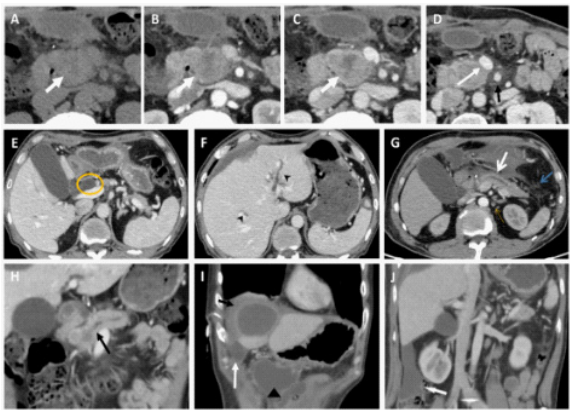

Figure 3: (a,b,c). The abdominal enhanced CT showed focal irregular mass in the head of pancreas (white arrows), with a maximum of 46 X 32mm, the CT value was 54 Hu in plain scan, 63 Hu in arterial phase and 85 Hu in venous phase. After contrast enhancement, the density was lower than the surrounding pancreatic tissue, with delayed reinforcement.
(D). Axial CT image shows the superior mesenteric vein (SMV) (white arrow) is of regular caliber, with no circumferential vessel narrowing, occlusion, and vessel deformity (SMV teardrop-shaped deformity was negative). The SMA (black arrow) relative to the SMV with a ratio smaller than 1.0. Note there is no loss of fat in the perivascular space.
(E,F). Axial CT image shows the widest diameter of the CBD (E, yellow circle) was about 19 mm, accompanied by intrahepatic cholangiectasis (F, black short arrows).
(G). The pancreatic body and tail were slightly atrophied. Peripancreatic fat space was not clear, surrounding multiple bands and patchy shadows (blue arrow) and enlarged lymph nodes (yellow arrow). The main pancreatic duct was slightly expanded, about 5mm in width (black arrow).
(G,H). Coronal and Axial CT image show a duct-to-parenchyma ratio (maximum diameter of the diffusely dilated main pancreatic duct and the overlying slightly atrophic parenchyma) of smaller than 0.34.
(I,J). Coronal CT image shows Encapsulated effusions were formed in the right subphrenic space (I, black arrow), lacune neighboring the right colon (J, white arrow) and anterior abdominal wall (I, black triangle).

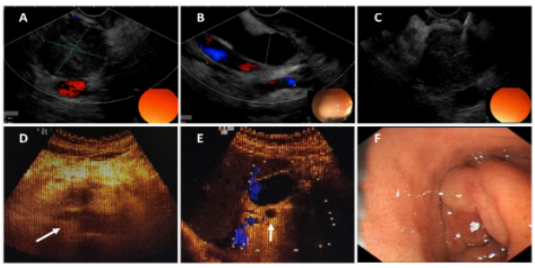

Figure 4: (A). Ultrasonic gastroscopy found a 33×36mm hypoechoic mass of the head of the pancreas at duodenal bulb and descending part, with clear boundaries.
(B). The common bile duct was dilated significantly, with a diameter of about 16mm.
(C). Under the guidance of ultrasound gastroscope, a 22G puncture needle was inserted into the tumor for several stitches and obtained several biopsies.
(D). Abdominal ultrasonography showed irregular pancreas shape, enlarged pancreatic head, and an irregular hypoechoic nodule with unclear boundary.
(E). The echo of parenchyma was uniform, and the width of main pancreatic duct was about 4.3 mm.
(F). Gastroscopy revealed a narrow duodenal bulb caused by mass compression.

Discussion

Gallstone disease (approximately 50%) and alcohol consumption (approximately 20%) are the most frequent causes of acute pancreatitis [7]. However, there is a considerable number of cases (approximately 25%) in the group of idiopathic acute pancreatitis in which no etiology can be found after routine diagnostic work-up (i.e., medical history, laboratory investigations, and imaging examination). The difficulty in revealing early malignant tumors can also lead to recurrent obstructive pancreatitis [8]. In the case presented here, the patient had recurrent acute pancreatitis without any common history leading to this condition (alcoholism, hyperlipidemia, gallstone disease, autoimmune pancreatitis, etc.). In addition, a mass of pancreatic head was formed during just a few months, accompanied by biliary obstruction and increase in the level of tumor marker CA19-9, which made the diagnosis more difficult and required multiple modal imaging examinations and even pathological biopsies.

MFCP is a protracted pancreatic inflammation that results in the fibrotic replacement of the destroyed pancreatic parenchyma and formation of a local mass due to chronic inflammatory cell infiltration, and a history of pancreatitis is an independent risk factor for MFCP [9,10]. No large studies have described the incidence of the mass-forming type in patients with chronic pancreatitis, but based on clinical experience, the incidence may not exceed 10-20% [11]. Causing stenosis of the common bile duct, the pancreatic duct, and the duodenum, as well as vascular encasement, the inflammatory mass in the pancreatic head is seen as the pacemaker of chronic pancreatitis, which is the site of predominant occurrence of PC [12,13]. Because CP is an independent risk factor for pancreatic cancer, MFCP is highly similar to PC, and the overlap between their clinical and imaging features renders their early preoperative and differential diagnosis challenging [14,15].

The typical feature of MFCP in multidetector CT is a hypoattenuating mass on unenhanced CT, which is hypovascular on contrast-enhanced scans (Figure 3A-C). These masses are usually hypointense on T1-weighted MRI (long-T1WI signal) and iso- to hyperintense on T2-weighted MRI (equal-long T2WI signal). MFCP is hypointense on arterial phase MRI, with moderate enhancement on venous phase scans, showing moderate hypointensity to isointensity in later phases [5,16]. All these imaging features are very similar between MFCP and PC. The head mass of the pancreas in this case showed the above features on CT and MRI, and the SUVmax values of 18-FDG-PET/CT were also high. On 18-FDG-PET/CT, most PCs show high uptake of 18F-FDG by localized lesions in the early and delayed phases, while some studies have described that inflammation can give rise to focal FDG uptake in the same intensity range as that in PCs, and there is a considerable overlap between the SUVmax values among these two diseases [17,18]. Therefore, it is not sufficient to diagnose PC based on the high uptake of 18- FDG on PET/CT.

In this case, the overlap between MFCP and PC imaging features was vividly displayed, but careful observation revealed the differences. The imaging feature of dilatation in both ductal systems (distal pancreatic duct and common bile duct) is known as a double-duct sign, which favors the diagnosis of a malignancy. Classically, the double-duct sign is seen in up to 80% of pancreatic head PCs; however, this sign is non-specific and can develop secondary to inflammatory processes in the pancreas

as well as in other non-malignant conditions [3,11]. Parenchymal calcifications, pseudocysts, and beaded pancreatic ducts are commonly seen in patients with CP, which should raise the possibility that a focal mass represents focal inflammatory change [5]. PC usually causes abrupt narrowing or even complete obstruction of the pancreatic duct, whereas an inflammatory mass most often results in gradual stenosis, which allows visualization of the pancreatic duct throughout the mass. This is called "duct-penetrating sign," which is 96% specific for an inflammatory pancreatic mass, with sensitivity of 85% and accuracy of 94%, and is best seen in MRCP [19,20]. In addition to the above typical imaging features of PC and MFCP, marked upstream pancreatic ductal dilatation with marked parenchymal atrophy are the other imaging hallmarks of PC. A pancreatic duct-to-parenchyma ratio greater than 0.34 also strongly favors the diagnosis of PC and determines the degree of a chance for malignancy. Relatively mild ductal dilatation with mild upstream parenchymal atrophy (pancreatic duct-to-parenchyma ratio, <0.34) raises the possibility of an inflammatory non-neoplastic cause [21]. At the same time, soft-tissue attenuation that encases the adjacent vasculature is highly suggestive of the extraglandular spread of PC [22]. Circumferential vessel narrowing, occlusion, and vessel deformities partly indicate malignancy. Enlargement of the SMA relative to the SMV with a ratio greater than or equal to 1.0 is an additional sign favoring the diagnosis of malignancy rather than an inflammatory process in the pancreas [23]. Although MDCT and MRCP manifest positive "double-duct sign", and "duct-penetrating sign" was negative in this case, there were no pancreatic parenchymal calcifications and beaded pancreatic duct dilatation. At the same time, the pancreatic duct-to-parenchyma ratio was lower than 0.34, and no apparent abnormality was found in the mesenteric vessels (Figure 3G,H). There was a collateral branch duct dilatation in the distal pancreas in this case, which was thought to be secondary to a traction effect from fibrosis in a patient with chronic pancreatitis, rather than a mass effect from a neoplasm, where duct obliteration would be expected [24].

The patient in this case was initially misdiagnosed with PC. During the laparotomy, it was found that the tissue around the pancreatic head was closely adherent to the mesenteric vessels; the pancreaticoduodenectomy was stopped, and some suspicious tissues were taken for pathological biopsy. The results showed chronic inflammatory cell infiltration and fiber hyperplasia. Two months after the operation, the patient developed painless jaundice and elevated CA19-9 levels. A meta-analysis suggests that elevated CA19-9 by itself is insufficient for differentiating pancreatic carcinoma and chronic pancreatitis; however, it increases a suspicion of pancreatic carcinoma and needs to complement other clinical findings to improve diagnostic accuracy [25]. Pathological biopsy is the most convincing evidence for differentiation. Some studies suggest that contrast-enhanced EUS-FNA can help identify hypoenhanced hypovascular areas for targeted biopsy and identify areas of probable necrosis [26]. After that, EUS-FNA was performed, and the results of cytology and tissue section biopsy suggested chronic inflammation changes without evidence of malignant cells. Finally, the diagnosis of MFCP was clearly established. For patients with MFCP who have no chance of pancreaticoduodenectomy, obstructive jaundice, and impaired liver function, biliary stent implantation has therapeutic the significance for prognosis.

Conclusion

In summary, it is extremely difficult to diagnose atypical MFCP that mimics PC at clinical presentation, laboratory findings, and imaging features. This differentiation is important to avoid unnecessary resection in patients with inflammatory masses, especially in those with poor nutritional status. Multimodal imaging appears to be a feasible and useful method for the diagnosis of atypical MFCP. In the meantime, we propose that the combination of multimodal imaging and EUS-FNA may improve the diagnostic rate of atypical MFCP and avoid unnecessary surgery.

Author contributions: Han-Yue Wang collected and sorted out the data, as well as conceived and wrote the manuscript; Jie Peng performed the FNA for the patient; Hao-Su Huang and Meng Wang discussed the results together and contributed to the final manuscript; Jie Peng and Han-Yue Wang were responsible for the revision of the manuscript for important intellectual content; all authors issued final approval for the version to be submitted.

Ethics approval and consent to participate: All the procedures have been performed in accordance with the Helsinki Declaration of 1964 and later versions. This study was reviewed and approved by the Ethic Committee of the Xiangya Hospital of Central South University [approval number: 202012205]. Written informed consent was obtained prior to imaging allowing presentation of this case and data.

Consent for publication: The patient agreed to allow his case to be published including any relevant laboratory data and images, and written informed consent was obtained from the patient.

Informed consent statement: Informed written consent was obtained from the patient for publication of this report and any accompanying images.

Conflict-of-interest statement: The authors declare that they have no conflict of interest.

Acknowledgements: Not applicable.

Reference

1. Adamska A, Domenichini A, Falasca M. Pancreatic Ductal Adenocarcinoma: Current and Evolving Therapies. Int J Mol Sci. 2017; 22; 18: 1338.

2. Zakaria HM, Mohamed A, Alsebaey A, Omar H, ELazab D, Gaballa NK. Prognostic factors following pancreaticoduodenectomy for pancreatic ductal adenocarcinoma. Int Surg J. 2020; 5: 3877.

3. Klein F, Jacob D, Bahra M, Pelzer U, Puhl G, Krannich A, et al. Prognostic factors for long-term survival in patients with ampullary carcinoma: the results of a 15-year observation period after pancreaticoduodenectomy. HPB Surg. 2014; 2014: 970234.

4. Steer ML, Waxman I, Freedman S. Chronic pancreatitis. N Engl J Med. 1995; 332: 1482–1490.

5. Kim T, Murakami T, Takamura M, Hori M, Takahashi S, Nakamori S, et al. Pancreatic mass due to chronic pancreatitis: correlation of CT and MR imaging features with pathologic findings. AJR Am J Roentgenol. 2001; 177: 367–371.

6. Tajima Y, Kuroki T, Tsutsumi R, Isomoto I, Uetani M, Kanematsu T. Pancreatic carcinoma coexisting with chronic pancreatitis versus tumor-forming pancreatitis: diagnostic utility of the time-signal intensity curve from dynamic contrast-enhanced MR imaging.

World J Gastroenterol. 2007; 13: 858–865.

7. Nesvaderani M, Eslick GD, Vagg D, Faraj S, Cox MR. Epidemiology, aetiology and outcomes of acute pancreatitis: A retrospective cohort study. Int J Surg. 2015; 23: 68–74.

8. Bakker OJ, van Brunschot S, van Santvoort HC, Besselink MG, Bollen TL, et al. Early versus on-demand nasoenteric tube feeding in acute pancreatitis. N Engl J Med. 2014; 371: 1983–1993.

9. Braganza JM, Lee SH, McCloy RF, McMahon MJ. Chronic pancreatitis. Lancet. 2011; 377: 1184–1197.

10. Neff CC, Simeone JF, Wittenberg J, Mueller PR, Ferrucci JT. Inflammatory pancreatic masses. Problems in differentiating focal pancreatitis from carcinoma. Radiology. 1984; 150: 35–38.

11. Schima W, Böhm G, Rösch CS, Klaus A, Függer R, Kopf H. Mass-forming pancreatitis versus pancreatic ductal adenocarcinoma: CT and MR imaging for differentiation. Cancer Imaging. 2020; 20: 52.

12. Singh VK, Yadav D, Garg PK. Diagnosis and Management of Chronic Pancreatitis: A Review. JAMA. 2019; 322: 2422–2434.

13. Függer R, Gangl O, Fröschl U. Clinical approach to the patient with a solid pancreatic mass. Wien Med Wochenschr. 2014; 164: 73–79.

14. Ruan Z, Jiao J, Min D, Qu J, Li J, Chen J, et al. Multi-modality imaging features distinguish pancreatic carcinoma from mass-forming chronic pancreatitis of the pancreatic head. Oncol Lett. 2018; 15: 9735–9744.

15. Dutta AK, Chacko A. Head mass in chronic pancreatitis: Inflammatory or malignant. World J Gastrointest Endosc. 2015; 7: 258–264.

16. Srisajjakul S, Prapaisilp P, Bangchokdee S. CT and MR features that can help to differentiate between focal chronic pancreatitis and pancreatic cancer. Radiol Med. 2020; 125: 356–364.

17. Kato K, Nihashi T, Ikeda M, Abe S, Iwano S, Itoh S, et al. Limited efficacy of (18)F-FDG PET/CT for differentiation between metastasis-free pancreatic cancer and mass-forming pancreatitis. Clin Nucl Med. 2013; 38: 417–421.

18. Shreve PD. Focal fluorine-18 fluorodeoxyglucose accumulation in inflammatory pancreatic disease. Eur J Nucl Med. 1998; 25: 259–264.

19. Boninsegna E, Manfredi R, Negrelli R, Avesani G, Mehrabi S, Pozzi Mucelli R. Pancreatic duct stenosis: Differential diagnosis between malignant and benign conditions at secretin-enhanced MRCP. Clin Imaging. 2017; 41: 137–143.

20. Ichikawa T, Sou H, Araki T, Arbab AS, Yoshikawa T, et al. Duct-penetrating sign at MRCP: usefulness for differentiating inflammatory pancreatic mass from pancreatic carcinomas. Radiology. 2001; 221: 107–116.

21. Eloubeidi MA, Luz LP, Tamhane A, Khan M, Buxbaum JL. Ratio of pancreatic duct caliber to width of pancreatic gland by endosonography is predictive of pancreatic cancer. Pancreas. 2013; 42: 670–679.

22. Wolske KM, Ponnatapura J, Kolokythas O, Burke LMB, Tappouni R, et al. Chronic Pancreatitis or Pancreatic Tumor? A Problem-solving Approach. Radiographics. 2019; 39: 1965–1982.

23. Elmas N, Oran I, Oyar O, Ozer H. A new criterion in differentiation of pancreatitis and pancreatic carcinoma: artery-to-vein ratio using the superior mesenteric vessels. Abdom Imaging. 1996; 21: 331–333.

24. Busireddy KK, AlObaidy M, Ramalho M, Kalubowila J, Baodong L, Santagostino I, et al. Pancreatitis-imaging approach. World J Gastrointest Pathophysiol. 2014; 5: 252–270.

25. Su S-B, Qin S-Y, Chen W, Luo W, Jiang H-X. Carbohydrate antigen 19-9 for differential diagnosis of pancreatic carcinoma and chronic pancreatitis. World J Gastroenterol. 2015; 21: 4323–4333.

26. Seicean A, Badea R, Moldovan-Pop A, Vultur S, Botan EC, Zaharie T, et al. Harmonic Contrast-Enhanced Endoscopic Ultrasonography for the Guidance of Fine-Needle Aspiration in Solid Pancreatic Masses. Ultraschall Med. 2017; 38: 174–182.